17th International Conference on Greenhouse Gas Control Technologies, GHGT-17

20th -24th October 2024 Calgary, Canada

Calcium Looping for Decarbonizing Electric Arc Furnace Steelmaking with CCS: a preliminary analysis of the role of solid storage

Néstor D. Montiel-Bohórquez[a]*, Edoardo de Lena[b], Maurizio Spinelli[b], Malin Blomqvist[c], Paul Cobden[c], Manuele Gatti[a], Matteo C. Romano[a]

[a]*Politecnico di Milano, Department of Energy, via Lambruschini 4, 20156 Milan, Italy*
[b]*Laboratorio Energia e Ambiente Piacenza (LEAP), via Nino Bixio 27/C, 29121 Piacenza, Italy*
[c]*Swerin AB, Aronstorpsvägen 1, 97437 Luleå, Sweden*

Abstract

Decarbonising Electric Arc Furnace (EAF) steelmaking (30% of global steel production) is crucial to achieving the emission reduction targets in the iron and steel sector, which is responsible for ~7% of global energy-related CO_2 emissions. Carbon capture in EAF steelmaking is necessary to manage the unavoidable process emissions. However, the flue gases produced in the EAF have highly variable properties, making integrating carbon capture technologies within EAF plants particularly challenging.
In this work, process simulations are used to assess and compare various CaL plant configurations for capturing CO_2 from EAF flue gases. The CaL plant configuration with two intermediate solid storage vessels offers advantages, requiring smaller equipment sizes and lower resource consumption than the configuration with one intermediate solid storage vessel.

Keywords: Electric Arc Furnace steelmaking decarbonisation, carbon capture, Calcium Looping, variable properties flue gases.

1. Introduction

The iron and steel production sector contributes approximately 7% of the global direct CO_2 emissions from energy use [1]. Steel production methods involving the Electric Arc Furnace (EAF) technologies (scrap-EAF, DRI-EAF) account for roughly 30% of the global steel output, and its specific CO_2 emissions range between 0.15 and 1.08 t_{CO2}/t_{steel}. Of these emissions, around 19% are fuel-related, while the remaining 81% are classified as process emissions [2]. As a result, achieving deep decarbonisation in EAF steelmaking requires implementing CO_2 capture technologies to address the process emissions that cannot be mitigated by improving energy efficiency or substituting fossil fuels.

Among CO_2 capture technologies, Calcium Looping (CaL) has emerged as a promising option, mainly due to its suitability to be integrated with high-temperature industrial processes (e.g., cement, chemical, steel, and power production). Compared to more mature capture technologies (i.e., amine-based chemical absorption), CaL may achieve superior performance in these applications [3,4]. However, applying CaL for CO_2 capture in EAF steelmaking presents specific challenges due to the highly fluctuating properties of flue gases, which means that the CaL system should

* Corresponding author. Email address: nestordario.montiel@polimi.it

operate under fluctuating loads. To enhance flexibility and performance in handling variable-properties flue gases, the integration of intermediate solid storage within the CaL system has been proposed as a viable strategy [5–8].
This work, conducted within the framework of the EU-funded CaLby2030 project, focuses on applying the CaL system for CO_2 capture from EAF steelmaking. In particular, it considers a CaL plant utilising Circulating Fluidized Bed (CFB) reactors. The analysis involves process simulation and technical assessments of various CaL plant configurations, each incorporating strategies for managing the gas variability by adapting the solids circulation and storage systems.

Nomenclature

ASUS	Air separation unit
CFB	Circulating fluidised bed
CT	Cold tank
CPU	CO2 purification unit
EAF	Electric arc furnace
FBHE	Fluidized bed heat exchanger
F_{CO2}	Mole flow of CO2 in flue gas entering the carbonator [kmol/s]
F_{Ca}	Molar flow of sorbent (CaO) cycling to the carbonator [kmol/s]
HT	Hot tank
TES	Thermal energy storage

2. Calcium Looping applied to Electric Arc Furnace (EAF) steelmaking

2.1. EAF flue gases

Flue gases from EAF steelmaking exhibit highly variable properties due to the batch-based nature of the process. Each tap-to-tap cycle, typically lasting 50 – 90 minutes, includes phases of minimal (i.e., charging and tapping) and peak (i.e., melting, refining) flue gases production [9]. Figure 1 illustrates the key properties of the EAF flue gases analysed in this work—mass flow rate, CO_2 content, and temperature. The maximum gas flow rate (88 kg/s) is nearly two orders higher than the minimum (1 kg/s). Similarly, significant disparities are observed in CO_2 concentration, which peaks at 25 mol% and drops to 0%, and in temperature, reaching a high of 1,190 °C and a low of 100 °C. On average, the transition between these minimum and peak values spans approximately 25 minutes. Therefore, CO_2 capture systems applied to EAF steelmaking should be designed to deal with such fluctuations and ensure average capture levels according to mitigation targets and CO_2 quality specifications.

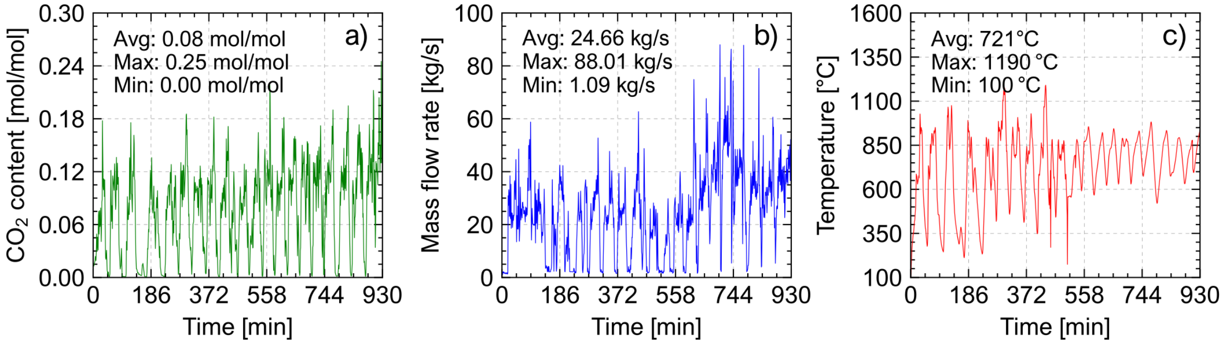

Figure 1. Profiles of EAF flue gas properties considered in this analysis: a) CO_2 content [mol/mol], b) mass flow rate [kg/s], c) temperature [°C].

2.2. CaL plant applied to EAF steelmaking

Figure 2 presents a schematic of the CaL plant applied to EAF steelmaking as end-of-pipe capture technology. The CaL plant is composed of five primary sub-systems: i) the EAF flue gas cooling section, ii) the calcium looping section (including calciner, carbonator and, optional, storage), iii) the CO_2 purification unit (CPU), iv) the air separation unit (ASU), and v) the thermal energy storage and steam cycle. Initially, the EAF flue gases are cooled to a temperature suitable (≤ 400 °C) for the fan, directing them to the carbonator. In the adiabatic carbonator operating at 620 °C, a CaO-based solid sorbent captures CO_2 from the gas phase through a heterogeneous reaction with CaO, forming $CaCO_3$, as described by Equation 1.

$$CaO_{(s)} + CO_{2\,(g)} \leftrightarrow CaCO_{3\,(s)} \qquad \Delta H_r^0 = -179.2\ kJ/mol \qquad (1)$$

As a result, CO_2-lean flue gas and carbonated solids exit the carbonator. The CO2-lean gas flows through the carbonator's convective pass for heat recovery before being discharged to the stack, while the carbonated sorbent is directed to the calciner. In the calciner, fuel combustion with high-purity oxygen (95 vol% from the ASU) raises the temperature to 920 °C, enabling complete sorbent regeneration by separating the CO_2 from the $CaCO_3$ [10]. The oxygen flow rate into the calciner is controlled so that the oxygen concentration at the outlet is 3.0 mol%. The regenerated sorbent is returned to the carbonator for a new CO_2 capture cycle, while the produced CO_2-rich gas is directed through the calciner's convective pass for heat recovery. The calciner fuel is residual forestry biomass with 51.0 wt.% C, 5.8 wt.% H, 0.9 wt.% N, 0.04 wt.% S, 38.21 wt.% O, 4.05 wt.% ash, and an LHV of 17.74 MJ/kg.

Following heat recovery, the CO_2-rich gas stream from the calciner is split into two branches: one portion recycles back to the calciner as a temperature moderator, and the other goes to the CO2-rich gas storage, and subsequently to the CPU for CO_2 dehydration, purification (via distillation) and compression [11]. The recycled CO_2-rich gas flow is controlled to maintain an oxygen concentration of 40 vol% at the calciner inlet. Recovered heat from the gas cooler and the convective passes of both reactors is used to drive a steam cycle, generating electric power. Part of this electricity powers the CO_2 capture plant (e.g., gas fans, ASU, CPU compressors, and pumps), while the surplus can be either exported for revenue or supplied to the EAF to reduce operating costs.

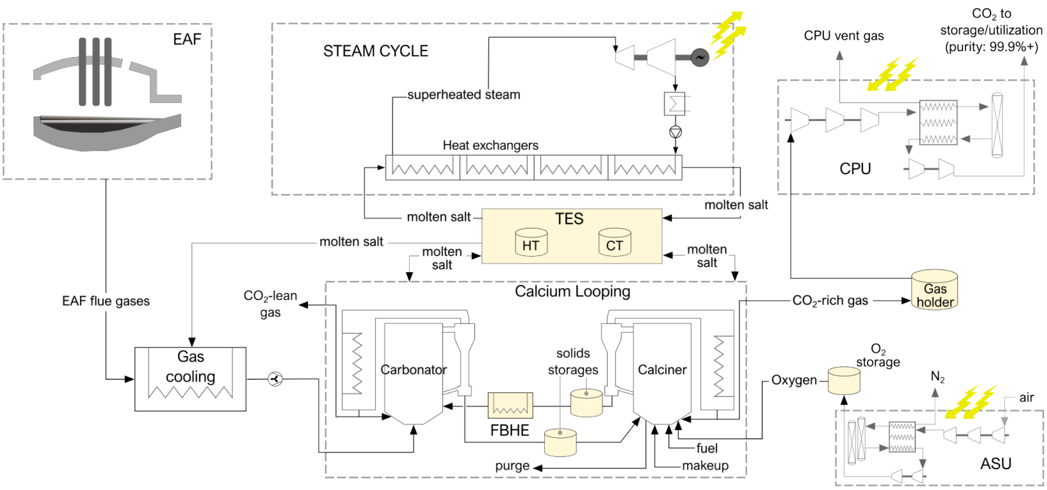

Figure 2. Scheme of the CaL plant applied to EAF steelmaking. It includes five main sub-systems: EAF flue gases cooling, CaL section, Air Separation Unit (ASU), CO_2 purification Unit (CPU), and Steam cycle.

To address the high variability of the flue gases, specific strategies are incorporated into the CaL plant to enhance its flexibility for CO_2 capture from EAF steelmaking. The plant components involved in these strategies are highlighted in the schematic shown in Figure 2, with detailed descriptions provided in Table 1.

Table 1. Description of the features implemented in the CaL capture plant to improve its capability to capture CO2 from the EAF gases with fluctuating properties.

Feature	Description
1. Carbonator gas recirculation	During periods with low EAF flue gas flow rate, a portion of CO_2-lean gases exiting the carbonator is recirculated back to the reactor to maintain an adequate volumetric flow rate in the riser. The recirculated flow rate is set to ensure a minimum superficial gas velocity of 3 m/s.
2. Adiabatic carbonator + external fluidised bed heat exchanger (FBHE)	In a typical carbonator, internal heat transfer surfaces regulate the reactor's temperature, with water or steam absorbing part of the thermal energy to maintain the desired reactor temperature. The heat transfer system must manage the sensible heat from solids arriving from the calciner at 920 °C and the heat released by the exothermal carbonation reaction. Effective control of carbonation temperature is essential, as it significantly influences CO_2 capture efficiency. In this application, however, the carbonator operates under variable conditions, with fluctuations in both the solids' flow rate and the heat generated by the carbonation, driven by changes in the EAF flue gas properties. Due to this, an adiabatic carbonator without internal heat transfer surfaces is considered in this work. Temperature control for the carbonator is managed through a fluidised bed heat exchanger (FBHE). This configuration has been reported to improve flexibility and system control since the heat extraction is separated from the reacting-capture process under variable conditions [5,8]. The solids' temperature at the FBHE outlet is set to have an average carbonator temperature of 620 °C, according to the solids and CO_2 flow rates. Temperature is controlled by regulating the bypass level of solids through the FBHE.
3. Intermediate solid storage	Previous studies have explored using intermediate solids storage to enhance the flexibility of the CaL system for CO_2 capture from variable CO_2 sources, such as power plants operating at partial load [5–8]. This approach places one or two vessels between the carbonator and the calciner to store solids. Solids exiting the carbonator with varying compositions are stored in a vessel, which is kept fluidised to avoid agglomeration issues and promote rapid mixing with the solid inventory in the vessel. This setup ensures that the solid´s composition at the vessel outlet is more uniform and allows precise control of the solids' flow rate to the calciner. As a result, the calciner, the ASU, and the CPU can operate under more stable and reduced loads variations, thereby lowering equipment costs. A detailed description of cases involving intermediate solids storage is provided in section 2.3.
4. Gas storage for oxygen from ASU and CO_2-rich gas to CPU	A gas storage unit is placed between the calciner and the ASU to store the oxygen produced by the ASU. This configuration enables the ASU to operate at a stable load by producing oxygen at a constant rate, independent of the calciner's variable oxygen demand. Oxygen is then supplied to the calciner according to the requirements for burning fuel to maintain an average calciner temperature of 920 °C. Similarly, a second gas storage is located between the calciner and the CPU to store the CO_2-rich gas produced in the calciner. The gas holder provides the CPU with a constant gas flow rate, allowing it to be designed for average rather than peak load and enabling stable load operation of the compressors.
5. Thermal energy storage (TES) between the CaL section and the power block	In the CaL plant, heat is recovered from multiple sources: EAF flue gases, carbonator flue gas, CO_2-rich gas from the calciner, and solids in the FBHE. The recovered heat is used to produce steam, which is expanded in a turbine to generate power. In this work, a thermal energy storage (TES) system is employed to decouple the steam cycle operation from the fluctuation in the heat sources. The TES system comprises two tanks to store hot and cold molten salt (Nitrate salt, 60 %wt NaNO3 – 40 %wt KNO3), the selected heat transfer fluid. This heat transfer fluid is selected because of its high maximum operating temperature of 550 °C [12], which benefits the steam cycle thermal efficiency. Cold molten salt at 265 °C is directed to the various heat recovery points at variable flow rates, depending on the available heat, and the resulting hot molten (540 °C) salt is stored in the hot tank. This configuration provides a stable thermal input to the steam cycle by supplying molten salt at a constant flow rate and temperature, avoiding transient operation and preventing the steam cycle from being subjected to frequent load changes.

2.3. Different plant configurations

Four different plant configurations (cases) are analysed. In all cases, the plant includes the five subsystems described in Section 2.2. Additionally, most strategies described in Table 1 are common across all configurations. Nonetheless, they differ from, first, the presence (or absence) of intermediate solid storage between the carbonator and calciner in the CaL section and, second, in the number of solid storage vessels (one or two) (Figure 3).

In the first case (Figure 3a) no intermediate solid storage is included. Moreover, the solids circulation between the reactors is adjusted based on the CO_2 flow entering the carbonator and the energy balance of the carbonator, which operates at a constant temperature of 620 °C. When the CO_2 flow is sufficiently high (and the heat released from the carbonation reaction can maintain 620 °C), the solids flow rate into the carbonator is adjusted to ensure a minimum sorbent (CaO) to CO_2 molar ratio (F_{Ca}/F_{CO2})- of 8. Conversely, when the CO_2 flow is low, the solids flow rate is increased to provide additional energy to the reactor through the sensible heat of the solids. This case is labelled "no storage, variable solid circulation" (NST-V) and is the baseline for comparing the other cases.

The second case (Figure 3b), like NST-V, does not include intermediate solid storage. However, the solids circulation between the reactors is kept constant to reduce the variability in the solids' composition exiting the carbonator. The constant solids flow rate is determined based on the maximum CO_2 flow entering the carbonator to achieve an F_{Ca}/F_{CO2} of 8. This case is labelled "no storage, constant solid circulation" (NST-C).

In the third case (Figure 3c), an intermediate solid storage unit is included to store the solids coming from the carbonator. The solid circulation between the reactors is kept constant. Additionally, the solid inventory within the storage unit is maintained constant by balancing the solids flow rate out of the storage with the incoming flow from the carbonator ($m_{solid,\ out} = m_{solid,\ in}$). The storage volume (solid inventory) is sized to ensure that the minimum partial load (i.e., fuel input and O_2 consumption) in the calciner island remains at 70% of the on-design load. This case is labelled "one storage, constant solid circulation (1ST-C).

In the fourth case, two solid storage units are included to store solids exiting the carbonator and the calciner, respectively. The solids circulation between the reactors is variable. The first storage unit receives solids from the carbonator at a variable rate, based on the incoming CO_2 flow, and supplies solids to the calciner at a constant (average) rate; as a result, the calciner island is designed considering the average solid flow rate. Similarly to 1ST-C, the storage solid inventory is sized to ensure that the minimum load for the calciner island remains at 70% of the on-design load. The second storage vessel receives solids from the calciner (at a constant rate) and provides them to the carbonator at a variable rate, depending on the CO_2 input and the sensible heat required to maintain the carbonator temperature. Consequently, the solids inventory in the vessel changes over time as the inflow rate differs from the outflow rate. This case is labelled "two storages" (2ST).

2.4. Components design and operation.

Given the fluctuations in flue gases to be processed in the CaL plant, the design and sizing of its various components is not trivial. For instance, the design point can be defined to maximise system performance (CO_2 capture efficiency) or based on a trade-off between performance and economic indicators. This work focuses on analysing the application of CaL to EAF steelmaking and comparing different configurations to achieve high CO_2 capture efficiencies in the carbonator (>90% of CO_2 in EAF flue gases). Consequently, the components of the plant are designed to accommodate the most critical conditions (e.g. max flow rate, min CO_2 concentration, etc.) based on the properties of the EAF flue gas (Figure 1).

The EAF flue gases cooler is designed to reduce the temperature of 81.7 kg/s of EAF flue gas from 930 °C to 400 °C, handling a thermal load of 51 MW. Molten salts, used as the cooling fluid, enter the cooler at 265 °C and exit at 540 °C. The required heat transfer surface area is computed using the Thermoflex package, and the result is 2,070 m^2.

A superficial gas velocity range of 3 to 7 m/s is established for the carbonator design, consistent with typical conditions for CFB systems [13]. The riser cross-section area is sized based on the maximum gas volumetric flow rate of 224 m^3/s at 620 °C and the highest gas velocity of 7 m/s. For conditions with lower volumetric flow rates, the superficial gas velocity is maintained within the 3-7 m/s range; at very low flow rates, carbonator flue gas recirculation is employed to maintain the minimum gas velocity of 3 m/s. Although gas recirculation helped sustain the fluidisation regime in the carbonator riser, it also resulted in CO_2 dilution. The carbonator convective pass is designed, using Thermoflex, to cool a gas flow of 87.75 kg/s from 620 °C to 280 °C. Like in the EAF flue gas cooler, molten salts are used as the cooling fluid, entering at 265 °C and exiting at 540 °C. The estimated heat transfer surface area is 25,200 m^2.

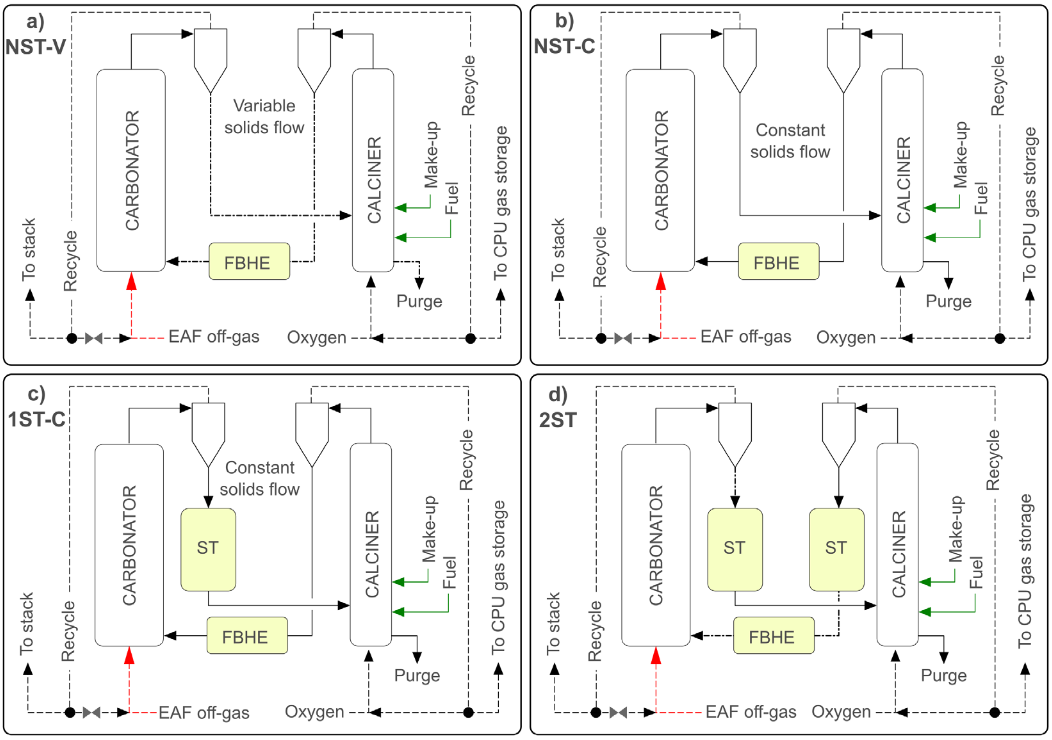

Figure 3. CaL section simplified layout for the different cases. Dashed lines are for gas streams, Dashed-dotted lines are for solids with variable flow rates, and black solid lines are for solids with constant flow rates.

The calciner and its convective pass are designed following a similar approach based on mass and energy balances obtained from simulations for each configuration (case). Additional details regarding the calciner's design and operational parameters are provided in Section 3.1. Similarly, the capacities of the gas storage units (O_2 and CO_2-rich gas), ASU, CPU, and steam cycle are determined based on results from simulated mass and energy balances.

2.5. Simulation strategy

Minutely average values are calculated for the key EAF flue gas properties, including mass flow rate, composition (CO_2, H_2O, O_2, N_2), and temperature, resulting in a dataset of 930 points. Each point reflects a distinct operating condition for the CaL plant. They are simulated to obtain the mass and energy balance of the system when processing the fluctuating EAF flue gas. 0D models are implemented for the different sections, following the design procedure described in Section 2.4. A set of assumptions are made to reduce the complexity of simulations while maintaining a sufficient accuracy level. These assumptions allowed a comparative analysis of the different cases considered (Section 2.3), enabling valid conclusions to be drawn regarding the advantages of each plant configuration.

- The carbonator captures 95% of the maximum possible CO_2, as dictated by the equilibrium of CO_2 at each simulation point. In addition, complete conversion of $CaCO_3$ to CaO and CO_2 is assumed in the calciner.

- Models of CaL reactors consider a single representative temperature, set as the average within each reactor under specified boundary conditions for each simulated point. These average temperatures are 620 °C for the carbonator and 920 °C for the calciner.
- Intermediate solid storage units are assumed to be fluidised beds operating at minimum fluidisation, where incoming solids mix instantly with the solid inventory in the vessel.
- Off-design operation is accounted for in each simulation point to evaluate the system's performance under conditions different from the on-design ones; however, the components' dynamic responses are not included at this stage. Thus, simulations are conducted assuming that each simulated point is an instantaneous quasi-steady state of the system.

Various tools are used to simulate the different sections of the CaL plant (Figure 4). For the CaL section, a model is implemented in Aspen Plus to reproduce the mass and energy balances of the carbonator and calciner. The heat recovery sections are first designed with Thermoflex. Once the on-design heat transfer area and configuration are defined, the off-design simulations are conducted using the Thermoflex's build-in routines for off-design operation analyses. The CPU is modelled in Aspen Plus following the high-purity configuration in [11], which produces CO_2 with a purity of 99.9% at 110 bar and 28 °C. The CPU model included dust abatement, dehydration, a cold box, a distillation unit, and CO_2 compression and liquefaction. Since the CO_2-rich gas storage maintains a constant load, no off-design simulations are needed for the CPU. A state-of-the-art cryogenic ASU is defined to produce oxygen for fuel combustion in the calciner. Thus, power consumption for oxygen production is sourced from [14] and no simulations of the ASU are conducted. Finally, the steam cycle components are designed and simulated using Thermoflex. Similarly to the CPU, no off-design simulation of the steam cycle is required since the TES provides a stable thermal input.

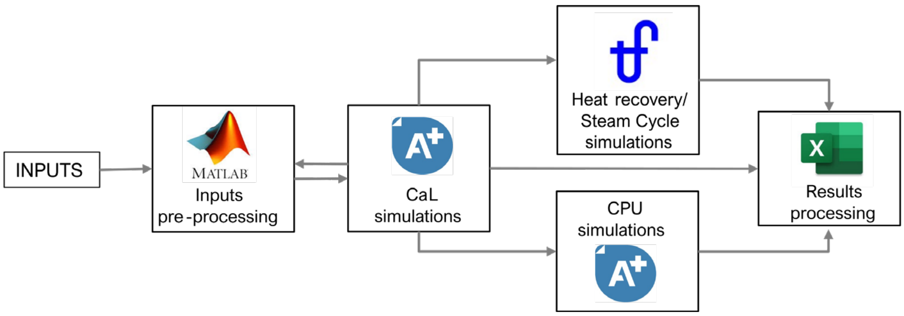

Figure 4. Blocks diagram for the modelling framework implemented to simulate the CaL plant applied to EAF steelmaking.

3. Results

3.1. The effect of intermediate solid storage

The profiles of $CaCO_3$ content in the solids stream entering (orange line) and exiting (black line) the storage for solids produced in the carbonator are depicted in Figure 5, for 1ST-C and 2ST. These profiles are obtained with solids inventories of 1,750 tons and 750 tons for 1ST-C and 2ST, respectively. The variability in the composition of solids is significantly reduced in both cases due to the buffering effect of the solid inventory in the storage vessels. For 1ST-C, the variability of $CaCO_3$ mass fraction changed from 0.00 – 0.19 kg/kg to the narrower range of 0.03 – 0.07 kg/kg. Similarly, for 2ST, it changed from 0.00 – 0.20 kg/kg to 0.09 – 0.16 kg/kg. The $CaCO_3$ concentrations for 1ST-C are lower because the solid mass flow rate (~150 kg/s) at the outlet of the storage vessel is higher when compared to 2ST (~54 kg/s), while the total mass of $CaCO_3$ from the carbonator is the same since the CO_2 capture efficiency is the same, under the assumptions made for the analysis. Also, it is important to note that the solid inventory in 1ST-C (1,750 tons) is more than two times that for 2ST (750 tons).

The operating profiles obtained for key calciner island parameters—fuel input, volumetric flow rate, oxygen consumption, and CO_2-rich gas sent to the CPU—are shown in Figure 6. Within each case, the four parameters have a similar profile due to their interdependency. The oxygen demand and CO_2-rich gas flowrate produced in the calciner are proportional to the fuel input under the constraint that the reactor temperature and oxygen composition at the outlet remain constant (i.e., there is a constant proportion between the amount of CO_2 to be extracted from calcination and the O_2 and fuel input if the calciner efficiency remains the same). Similarly, the volumetric flow rate in the calciner only depends on the oxidant mass flow rate (O_2 + recirculated CO_2-rich gas) since the calciner temperature is constant at 920 °C.

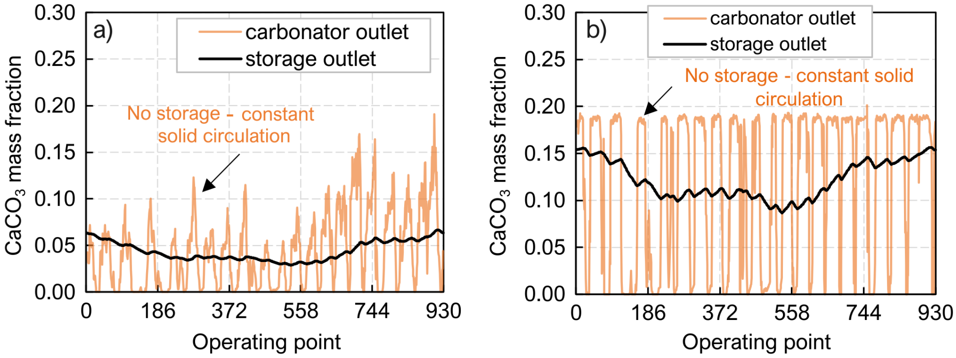

Figure 5. $CaCO_3$ compositions at the outlet of the carbonator (orange) and outlet of the vessel storing solid from the carbonator (black): a) case with one solid storage and constant solid circulation (1ST-C) with a solid inventory of 1,750 tons, b) case with two solid storages (2ST) with a solid inventory of 750 tons. Each operating point is related to a system simulation where corresponding values from Figure 1 are used as inputs. As indicated in each chart, the orange line also represents the $CaCO_3$ content profile at the calciner inlet: a) for NST-C and b) for NST-V.

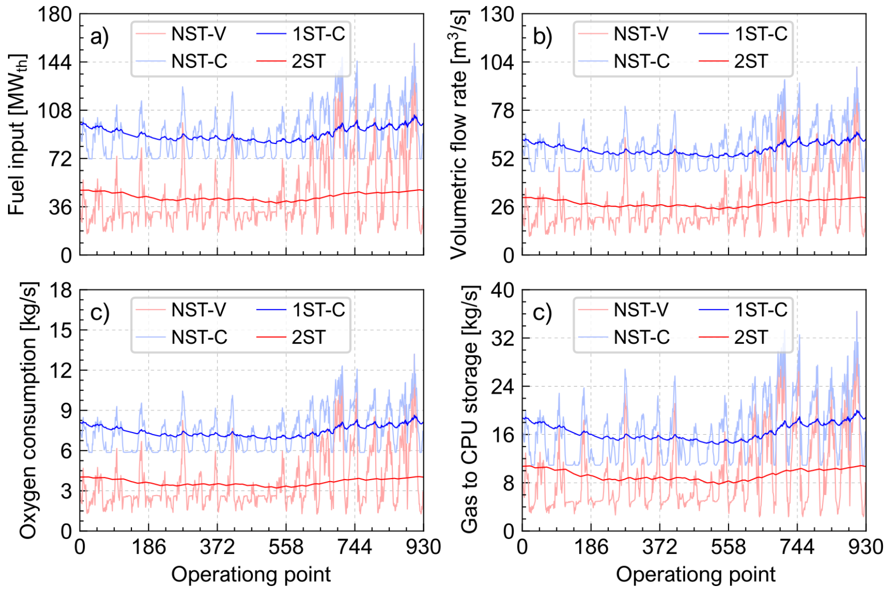

Figure 6. Profiles of relevant calciner island's parameters: a) Fuel input [MWth], b) Calciner volumetric flow rate [m^3/s], c) Calciner oxygen consumption [kg/s], and CO2-rich gas to CPU gas storage [kg/s]. **Legends:** NST-V: No solid storage, variable solid circulation between the CaL reactors, NST-C: No solid storage, constant solid circulation between the CaL reactors, 1ST-C: One solid storage, constant solid circulation, 2ST: Two solid storages. Each operating point corresponds to a system simulation where corresponding values from Figure 1 are used as inputs.

NST-V exhibited the highest fluctuations in calciner operation; essentially, the variability of the EAF flue gas properties is transferred to the calciner since the solids from the carbonator go directly to the calciner. Larger variability in the calciner island means larger volumes to store oxygen and CO_2-rich gas (Table 2) and issues with calciner fluidisation due to low superficial gas velocities. With the lowest volumetric flow rate in the calciner island (10 m^3/s), the superficial gas velocity is < 1 m/s. For NST-C, significant fluctuations are also observed; however, the ranges are narrower compared to NST-V. For this case, the superficial gas velocity in the calciner ranged from 3.1 to 7 m/s.

For 1ST-C and 2ST cases, the profiles are much more stable due to the buffering effect of solid storage on the composition of the solids fed to the calciner (see Figure 5). Nonetheless, 1ST-C consumes more fuel and oxygen (and requires a bigger CPU) due to the higher mass flow rate of solids that the calciner should process (150 kg/s vs 54 kg/s). Furthermore, for 1ST-C and 2ST, the peak capacities at which the components (reactors, ASU, and CPU) should be sized are lower, which means lower CAPEX requirement for these components.

3.2. Technical KPIs

Table 2 presents the average values for the main technical KPIs. Cases NST-V and 2ST led to equivalent average fuel and oxygen consumption, as well as similar CO_2 output from the CPU. This is because they processed the same amount of solids and captured the same amount of CO_2 over the analysed period. For the same reason, cases NST-C and 1ST-C had equivalent fuel consumption, oxygen demand, and CO2 output. However, the cases with constant solid circulation (NST-C and 1ST-C) consumed about twice as many resources because of the higher mass flow rate of solid recirculated between the reactors.

Under the assumptions applied, the CO_2 capture efficiency in the carbonator is the same across all cases. Even though NST-C and 1ST-C had a higher sorbent availability in the carbonator, the relative capture efficiency in the carbonator is assumed to be 95% of the maximum attainable capture efficiency dictated by the CO_2 equilibrium for all the cases.

Table 2. Average technical KPIs over the operating period analysed.

Parameter	NST-V	NST-C	1ST-C	2ST
Average fuel power input, [MW_{LHV}]	43.69	90.29	90.29	43.69
Average sorbent make-up consumption, [t/h]	3.29	9.47	9.47	3.29
Average O_2 consumption, [t/h]	13.09	26.81	26.81	13.09
Average CO_2 from the CPU to storage, [t/h]	25.4	42.9	42.9	25.4
CO_2 captured from EAF gas–fuel, [%]	39.0-55.6	23.0-67.9	23.0-67.9	39.0-55.7
Carbonator capture efficiency, [%]	90.81	90.81	90.81	90.81
Global capture efficiency, [%]	91.26	92.29	92.56	91.57
Specific fuel consumption, [MJ/kg_{CO2}][1]	15.04	31.08	31.08	15.04
Specific CO_2 production, [kg_{CO2}/kg_{CO2}][1,2]	1.57	3.35	3.35	1.57
Net CO_2 emissions, [t/h]	-12.50	-27.28	-27.41	-12.59
Steam cycle net power output, [MWe]	15.70	28.50	28.50	15.70
CaL plant net power output, [MWe]	5.98	12.82	10.06	4.42
Oxygen storage volume, [m^3]	17,100	12,000	6,000	3,800
CO_2-rich gas storage volume, [m^3]	53,600	44,600	21,900	14,600

[1] kg_{CO2} in the denominator refers to the amount of CO2 captured from the EAF flue gases.

[2] kg_{CO2} in the numerator refers to the amount of CO_2 produced from the fuel and limestone makeup.

All cases achieved negative net CO_2 emissions, as the CaL plant also captured the CO_2 in the fuel (biomass). NST-C and 1ST-C resulted in larger negative emissions due to higher fuel consumption. This aspect could be seen as beneficial, as it implies more atmospheric CO_2 removal. However, it also means that more resources (biomass, oxygen, etc.) are used to capture the same amount of CO_2.

The net power exported by the steam cycle mirrored the trends obtained for total fuel and oxygen consumption. Cases with constant solid circulation (NST-C and 1ST-C) yielded higher net power output in the steam cycle due to the increased thermal input from the larger fuel consumption. On the other hand, the net power output from the CaL plant (after subtracting the auxiliary power for CPU, fans, ASU, and pumps) is lower for the cases with solid storage (1ST-C and 2ST) due to the additional electricity consumed by the fans required to maintain fluidisation in the solid storage vessels.

4. Conclusions

Applying CaL for CO_2 capture in EAF steelmaking was assessed from a technical perspective using process simulation. Different CaL plant configurations were analysed with and without intermediate solids storage to capture CO_2 from EAF flue gases with variable properties (flow rate, CO_2 concentration, and temperature). Results indicated that implementing intermediate solids storage (one or two storing vessels) significantly reduced operating variability within the calciner island. However, the configuration with one solid storage (1ST-C) required larger solids storage capacities (1,750 tons vs 750 tons) and greater calciner island capacities (50-100%) compared to the configuration with two solids storage vessels (2ST). This suggests that the 2ST configuration may be more efficient due to the reduced resource consumption (OPEX) and lower equipment capacity requirements (CAPEX). Nevertheless, an economic analysis is required to confirm this, as the higher electricity output and potential carbon credits revenues from 1ST-C (due to increased biomass combustion in the calciner) could offset the higher CAPEX.

Acknowledgements

The authors acknowledge the financial support from the CaLby2030 project that has received funding from the European Union´s Horizon Europe Research and Innovation program under grant agreement No. 101075416. Views and opinions expressed are, however, those of the author(s) only and do not necessarily reflect those of the European Union or European Climate, Infrastructure and Environment Executive Agency (CINEA). Neither the European Union nor the granting authority can be held responsible for them.

The authors would like to thank Sumitomo SHI FW (SFW) and Swerim AB for their contribution to the site measurements that led to the EAF flue gas data used in this study.

References

[1] International Energy Agency. Iron and Steel Technology Roadmap – Analysis - IEA. 2020.
[2] Kirschen M, Risonarta V, Pfeifer H. Energy efficiency and the influence of gas burners to the energy related carbon dioxide emissions of electric arc furnaces in steel industry. Energy 2009;34:1065–72. https://doi.org/10.1016/J.ENERGY.2009.04.015.
[3] Cormos CC. Evaluation of reactive absorption and adsorption systems for post-combustion CO2 capture applied to iron and steel industry. Appl Therm Eng 2016;105:56–64. https://doi.org/10.1016/J.APPLTHERMALENG.2016.05.149.
[4] Voldsund M, Gardarsdottir SO, De Lena E, Pérez-Calvo JF, Jamali A, Berstad D, et al. Comparison of Technologies for CO2 Capture from Cement Production—Part 1: Technical Evaluation. Energies 2019, Vol 12, Page 559 2019;12:559. https://doi.org/10.3390/EN12030559.
[5] Criado YA, Arias B, Abanades JC. Calcium looping CO2 capture system for back-up power plants. Energy Environ Sci 2017;10:1994–2004. https://doi.org/10.1039/C7EE01505D.
[6] Hanak DP, Biliyok C, Manovic V. Calcium looping with inherent energy storage for decarbonisation of coal-fired power plant. Energy Environ Sci 2016;9:971–83. https://doi.org/10.1039/C5EE02950C.
[7] Astolfi M, De Lena E, Casella F, Romano MC. Calcium looping for power generation with CO2 capture: The potential of sorbent storage for improved economic performance and flexibility. Appl Therm Eng 2021;194:117048. https://doi.org/10.1016/J.APPLTHERMALENG.2021.117048.

[8] Astolfi M, De Lena E, Romano MC. Improved flexibility and economics of Calcium Looping power plants by thermochemical energy storage. International Journal of Greenhouse Gas Control 2019;83:140–55. https://doi.org/10.1016/J.IJGGC.2019.01.023.

[9] Gandt K, Meier T, Echterhof T, Pfeifer H. Heat recovery from EAF off-gas for steam generation: analytical exergy study of a sample EAF batch. Ironmaking & Steelmaking: Processes, Products and Applications 2016;43:581–7. https://doi.org/10.1080/03019233.2016.1155812.

[10] De Lena E, Spinelli M, Martínez I, Gatti M, Scaccabarozzi R, Cinti G, et al. Process integration study of tail-end Ca-Looping process for CO2 capture in cement plants. International Journal of Greenhouse Gas Control 2017;67:71–92. https://doi.org/10.1016/J.IJGGC.2017.10.005.

[11] Magli F, Spinelli M, Fantini M, Romano MC, Gatti M. Techno-economic optimization and off-design analysis of CO2 purification units for cement plants with oxyfuel-based CO2 capture. International Journal of Greenhouse Gas Control 2022;115:103591. https://doi.org/10.1016/J.IJGGC.2022.103591.

[12] Pan CA, Ferruzza D, Guédez R, Dinter F, Laumert B, Haglind F. Identification of optimum molten salts for use as heat transfer fluids in parabolic trough CSP plants. A techno-economic comparative optimization. AIP Conf Proc 2018;2033. https://doi.org/10.1063/1.5067028/1023330.

[13] Ylätalo J, Ritvanen J, Tynjälä T, Hyppänen T. Model based scale-up study of the calcium looping process. Fuel 2014;115:329–37. https://doi.org/10.1016/J.FUEL.2013.07.036.

[14] Queneau PE, Marcuson SW. Oxygen pyrometallurgy at copper cliff - A half century of progress. JOM 1996;48:14–21. https://doi.org/10.1007/BF03221355/METRICS.